Morphological and LSU rDNA sequence variation within the *Gonyaulax spinifera–Spiniferites* group (Dinophyceae) and proposal of *G. elongata* comb. nov. and *G. membranacea* comb. nov.

MARIANNE ELLEGAARD[1]*, NIELS DAUGBJERG[2], ANDRÉ ROCHON[1]†, JANE LEWIS[1] AND IAN HARDING[3]

[1]*Phytosciences Research Group, School of Biosciences, University of Westminster, 115 New Cavendish Street, London W1W 6UW, UK*

[2]*Department of Phycology, Botanical Institute, University of Copenhagen, Øster Farimagsgade 2D, DK-1353 Copenhagen K, Denmark*

[3]*School of Earth and Ocean Sciences, Southampton Oceanography Centre, University of Southampton, European Way, Southampton SO14 3ZH, UK*

M. ELLEGAARD, N. DAUGBJERG, A. ROCHON, J. LEWIS AND I. HARDING. 2003. Morphological and LSU rDNA sequence variation within the *Gonyaulax spinifera–Spiniferites* group (Dinophyceae) and proposal of *G. elongata* comb. nov. and *G. membranacea* comb. nov. *Phycologia* 42: 151–164.

Cultures were established from cysts of the cyst-based taxa *Spiniferites elongatus* and *S. membranaceus*. Motile cells and cysts from both cultures and sediment samples were examined using light and scanning electron microscopy. The cyst–theca relationship was established for *S. elongatus*. The motile cells have the tabulation pattern 2 pr, 4′, 6″, 6c, ≥ 4s, 6‴, 1p, 1‴′, but they remain unattributable to previously described *Gonyaulax* species. There was large variation in process length and process morphology in cysts from both cultures and wild samples and there was variation in ornamentation and in the development of spines and flanges in motile cells. A new combination, *G. elongata* (Reid) Ellegaard *et al. comb. nov.* is proposed, following new rules of the International Code of Botanical Nomenclature that give genera based on extant forms priority over genera based on fossil forms. Extreme morphological variation in the cyst and motile stages of *S. membranaceus* is described and this species is also transferred to the genus *Gonyaulax*, as *G. membranacea* (Rossignol) Ellegaard *et al. comb. nov.* Approximately 1500 bp of large subunit (LSU) rDNA were determined for these two species and for *G. baltica*, *G.* cf. *spinifera* (= *S. ramosus*) and *G. digitalis* (= *Bitectatodinium tepikiense*). LSU rDNA showed sequence divergences similar to those estimated between species in other genera within the Gonyaulacales; a phylogeny for the Gonyaulacales was established, including novel LSU rDNA sequences for *Alexandrium margalefii*, *A. pseudogonyaulax* and *Pyrodinium bahamense* var. *compressum*. Our results show that motile stages obtained from the germination of several cysts of the 'fossil-based' *Spiniferites* and *B. tepikiense*, which were previously attributed to '*Gonyaulax spinifera* group undifferentiated', belong to distinct species of the genus *Gonyaulax*. These species show small morphological differences in the motile stage but relatively high sequence divergence. Moreover, this group of species is monophyletic, supported by bootstrap values of 100% in parsimony and maximum likelihood analyses.

INTRODUCTION

More than 200 species of living marine dinoflagellates are known to produce resting stages (cysts) as part of their life history (Head 1996). Many of these species have two names because the cyst and motile stage were described and named independently of one another by palynologists and phycologists, respectively. One important group of modern dinoflagellates is represented by the cyst-based genus *Spiniferites* Mantell, which comprises some 89 species, 31 subspecies and three varieties (Williams *et al.* 1998). So far, all tested *Spiniferites* cysts have germinated to produce a motile stage belonging to the genus *Gonyaulax* Diesing, with most studies referring the motile stage to *G. spinifera* (Claparède & Lachman) Diesing or the '*Gonyaulax spinifera* group' (Lewis *et al.* 1999). The latter was defined by Kofoid (1911) as com-

prising *G. spinifera*, *G. digitalis*, *G. diegensis* Kofoid and *G. triacantha* Jørgensen. Motile stages of cysts from the genera *Impagidinium* Stover & Evitt, *Nematosphaeropsis* Deflandre & Cookson, *Ataxiodinium* Reid, *Pentadinium* Gerlach, *Tectatodinium* Wall and *Bitectatodinium* Wilson have also been assigned to the *G. spinifera* group (Head 1996 and references therein; Lewis *et al.* 1999 and references therein). For many years, it has puzzled researchers that cysts with such different morphologies all apparently germinated into the same, or very similar, motile stages (e.g. Dale 1983). This situation gave rise to a debate over whether the motile stages were underclassified or the cysts overclassified. Recent work on four species in the *G. spinifera* group (Lewis *et al.* 1999, 2001; Ellegaard *et al.* 2002) has demonstrated that, although the motile cells of these species are similar, there are morphological differences that warrant assignment to separate species.

In this paper, we examine in detail the two cyst-based taxa *S. elongatus* Reid and *S. membranaceus* (Rossignol) Sarjeant with regard to the morphology of both the cyst and the motile stages; in addition, we determine *c.* 1500 bp at the 5′ end of the nuclear large subunit (LSU) rDNA (which includes highly variable domains) of four species of *Gonyaulax* that produce

* Corresponding author (me@bot.ku.dk). Present address: Department of Phycology, Botanical Institute, University of Copenhagen, Øster Farimagsgade 2D, DK-1353 Copenhagen K, Denmark.

† Present address: Geological Survey of Canada (Atlantic), PO Box 1006, Dartmouth, Nova Scotia, B24 4A2, Canada.

Table 1. Names and authors of the species of *Gonyaulax* examined, based on their motile stages and cysts.

Biological taxon	Cyst-based taxon
G. baltica Ellegaard *et al.*	
G. membranacea (Rossignol) Ellegaard *et al. comb. nov.*	*Spiniferites membranaceus* (Rossignol) Sarjeant
G. digitalis (Pouchet) Kofoid	*Bitectatodinium tepikiense* Wilson
G. elongata (Reid) Ellegaard *et al. comb. nov.*	*S. elongatus* Reid
G. cf. *spinifera* (Claparède & Lachman) Diesing	*S. ramosus* (Ehrenberg) Mantell

Spiniferites cysts and one *Gonyaulax* (*G. digitalis*) that produces cysts referable to *B. tepikiense*. In our phylogenetic analyses, the rDNA sequences of the five *Gonyaulax* species were put into the context of sequences from other species within the order Gonyaulacales, including three new sequences. We use the names of the motile stages wherever possible in this paper, but both sets of names, including authors, are cited in Table 1.

MATERIAL AND METHODS

Isolation, culture and microscopy

Cysts of *G. elongata* were isolated from surface sediment samples collected from Kirkwall Bay (The Orkney Islands, Scotland, UK), Bedford Basin (Nova Scotia, Canada), Disco Bay (Greenland), Faxafloi (Iceland), and the British North Sea coast. Further information on sampling locations, where available, can be obtained from the corresponding author. One hundred and twenty-seven cysts were isolated, of which eight germinated and six cultures were established, viz. one from the Bedford Basin, two from the Orkney Islands and three from the English North Sea coast. All cultures were slow growing and most were short-lived. Encystment took place spontaneously in all strains after 1–3 mo (Table 2). One *G. membranacea* cyst was isolated from surface sediment collected near Drogheda, Ireland, and this germinated to give a culture. Strain names and sources are listed in Table 2. Additionally, cysts of *G. membranacea* were isolated from surface sediment from Cornwall, south-west England, and those of *G. digitalis* from surface sediment from Bedford Basin, Canada. The cyst–theca relationships for *G. digitalis* and *G. membranacea* have been determined previously using material from these same sediment samples (Lewis *et al.* 1999, 2001); the cultures established for this study were used mainly for DNA sequence analyses.

Attempts were made to establish cultures from the cysts of

the other cyst-based genera that have been reported to germinate into motile *G. spinifera*–like cells, in order to include these in our phylogenetic analyses. We found few of these cysts and only specimens of *Impagidinium, Nematosphaeropsis* and *Tectatodinium* had cell contents. We were not able to establish cultures from any of these.

All sediment samples were kept cold (4°C) and dark until processing. Subsamples were rinsed with artificial sea water through 80 μm mesh onto 20 μm mesh. The 20–80 μm fraction was cleaned by ultrasonication and rinsed again onto the 20 μm sieve. Most of the sieved samples were density separated using sodium polytungstate, as described by Bolch (1997), at a specific gravity of 1.3. Individual cysts were isolated by micropipette into Corning microwells containing ~1.5 ml of f/2⁺-Si (Guillard 1973), after rinsing in drops of clean medium. The microwells were kept at 16°C, 14 : 10 h light–dark and examined for germinated cysts every few days for the first 2 wk and thereafter at irregular intervals. When a microwell contained *c.* 10 motile cells, they were transferred to a 50 ml Petri dish containing ~20 ml of f/2⁺-Si and from there to 100 ml conical flasks with 50 ml of f/2⁺-Si.

Cysts and motile cells for microscopical examination were fixed in Petri dishes with a drop of buffered formalin. For light microscopy (LM), motile cells were examined with an Olympus BH-2 microscope under bright field and Nomarski differential interference contrast, and under UV light using the fluorochrome calcofluor white (Fritz & Treimer 1985; calcofluor white was obtained from American Cyanamid, Bound Brook, New Jersey) to stain the thecal plates (Hansen 1993). Cysts of *G. membranacea* strain UW398 were also examined under LM using the Auto-montage image analysis software by Syncroscopy (Cambridge, UK) to produce single composite 2D images from 3D specimens (using a CCD camera and an Olympus BH-2 microscope connected to a frame grabber). For scanning electron microscopy (SEM), cysts or motile cells were pipetted into distilled water, cleaned with ultrasound, iso-

Table 2. Origins of strains and data on life cycle transitions.

Species	Origin	Processes of cysts produced in culture	Strain	Processes of original cyst	Germination	Encystment	Germination of new cysts
Gonyaulax elongata	Orkney	long; reduced	UW388	long	2 mo	1–3 mo	ND[1]
	Orkney		UW389	long	3 d	2.5 mo	7 d[2]
	Nova Scotia	long; like *Spiniferites frigidus*	UW408	reduced	6 mo[2]	2 mo	ND
	North Sea	long; reduced	UW410	reduced	14 d	1.5 mo	ND
	North Sea		UW411	reduced	13 d	1.5 mo	ND
	North Sea		UW412	long	13 d	1.5 mo	ND
G. membranacea	Drogheda		UW398	not applicable	2 wk	1.5 mo	none[2]

[1] ND = not determined.
[2] Left in 4°C and dark for approximately 3 mo.

Table 3. List of species included in the phylogenetic analyses. For some species, the sequence was determined for two strains, but in all cases the sequences were identical. The strain used for the analyses is underlined. The non-*Gonyaulax* strains were isolated from Danish waters, except *Pyrodinium bahamense* (The Philippines) and *Alexandrium catenella* (Monterey, California, USA).

Taxon	Strain	GenBank accession no.
A. catenella (Whedon & Kofoid) Balech	A3	AF200667
A. margalefii Balech	—	AY154957
A. pseudogonyaulax (Biecheler) Horiguchi *ex* Kita & Fukuyo	—	AY154958
Ceratium fusus (Ehrenberg) Dujardin	—	AF260390
C. lineatum (Ehrenberg) Cleve	—	AF260391
C. tripos (O.F. Müller) Nitzsch	—	AF260389
Fragilidium subglobosum (von Stosch) A.R. Loeblich	—	AF260387
Protoceratium reticulatum (Claparède & Lachmann) Bütschli	K-0485	AF260386
Pyrodinium bahamense var. *compressum* (Böhm) Steidinger *et al.*	JL37	AY154959
Gonyaulax baltica	UW394, UW396	AY154962
G. baltica	K-0487	AF260388
G. digitalis	UW415, UW416	AY154963
G. elongata	UW388	AY154964
G. cf. spinifera	UW323, UW341	AY154960
G. membranacea	UW413, UW414	AY154961
G. membranacea	UW398 (double checked)	AY154965
Outgroup		
Heterocapsa triquetra (Ehrenberg) F. Stein	K-0447	AF260401
Prorocentrum micans Ehrenberg	K-0335	AF260377

lated onto 8 μm nuclepore filters, dehydrated in a graded acetone series (20–100% in eight steps), dried with CO_2 in a critical point dryer (Polaron E3000 CPD), sputter-coated with gold using a Bio Rad Sc502, glued on to stubs and examined in a JEOL JSM-6400 SEM.

Newly formed cysts from strains UW389 and UW398 were individually isolated into microwells containing ~1.5 ml of f/2$^+$-Si, stored in the dark at 4°C for 3 mo and reintroduced to 16°C and 14:10 h light–dark for excystment. Only cysts from strain UW389 germinated successfully, but none resulted in new cultures (Table 2).

DNA extraction and sequence determination

Exponentially growing cultures were harvested by centrifugation at $2000 \times g$ for 10–20 min. The pellet was kept frozen for at least 2 d until DNA extraction was performed using the CTAB (2% hexadecyltrimethylammonium bromide) method (Doyle & Doyle 1987). Total DNA was precipitated with ethanol as described by Daugbjerg *et al.* (1994). The terminal primers D1R (Scholin *et al.* 1994) and 28-1483R (Daugbjerg *et al.* 2000) were used to amplify *c.* 1500 bp of the nuclear-encoded LSU rDNA gene (domains D1, D2 and D3+conserved core region; Lenaers *et al.* 1989). Terminal and three internal primers (see Hansen *et al.* 2000 for primer sequences) were used to determine the LSU rDNA sequences. Conditions for PCR amplification and thermal cycling are given by Hansen *et al.* (2000). Nucleotide sequences were determined using the Dye Terminator Cycle Sequencing Ready Reaction Kit (Perkin Elmer, Foster City, CA). Sequence reactions were run on an ABI PRISM™ 377 DNA sequencer (Perkin Elmer) according to the manufacturer's recommendations. GenBank accession numbers for the nine LSU sequences of the dinoflagellate species determined in this study are provided in Table 3.

Alignment and phylogenetic analyses

Information from the secondary structure of the ribosomal RNA was used to optimize the alignment (Wuyts *et al.* 2001).

The data matrix comprised 1453 bp, including introduced gaps; of these, 1119 bp were considered unambiguous and analysed using maximum parsimony (MP) and maximum likelihood (ML) methods. PAUP* version 4.0b8a (Swofford 1998) was applied for MP analysis with the heuristic search option and 1000 random addition of sequences and a branch-swapping algorithm (tree-bisection–reconnection). Characters were weighted equally and gaps treated as missing data. For ML analyses, Felsenstein's 84-model was invoked with empirical base frequencies; in our opinion, the topology of the *Gonyaulax* clade is so robust that it would not be altered by the use of other similar models. Bootstrap analyses with 1000 replications in MP and 100 replications in ML were conducted to determine the robustness of the clades (Felsenstein 1985). Two nongonyaulacalean thecate dinoflagellates, *Prorocentrum micans* and *Heterocapsa triquetra,* were used as an outgroup to polarize the ingroup comprising 16 gonyaulacalean taxa.

Other gonyaulacalean species were included in the LSU rDNA analysis to establish the position of the *Gonyaulax–Spiniferites* group within the order Gonyaulacales and to determine whether this group was monophyletic. *A. catenella* was included as the representative for the *A. tamarense* (Lebour) Balech complex. We were not able to include species of *Gonyaulax* without known *Spiniferites* cysts in the analyses.

RESULTS

In the most recent version of the International Code of Botanical Nomenclature (ICBN), the status of living genera vs fossil-based genera was clarified, giving priority to genera based on extant nomenclatural types (Greuter *et al.* 2000). The genus *Gonyaulax* (based on living material) therefore has priority over the fossil-based genus *Spiniferites,* even though the latter name is older. Therefore, we herein transfer the species *S. elongatus* and *S. membranaceus* to *Gonyaulax.* It seems
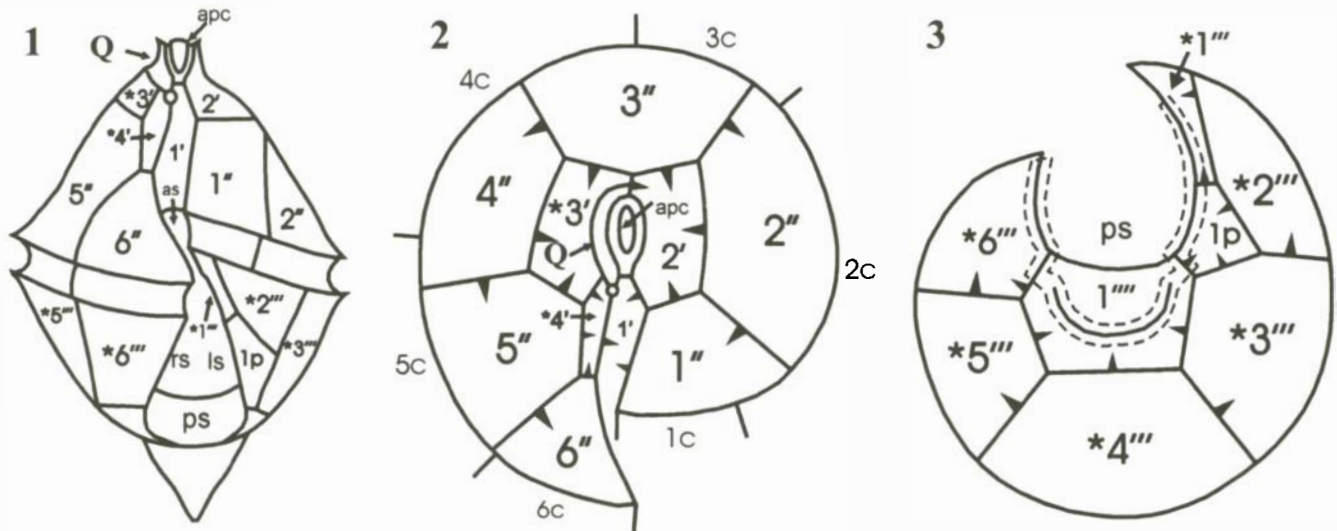
Figs 1–3. *Gonyaulax elongata*: line drawings of the tabulation of the motile cell. apc = apical pore complex. * = homologue.
Fig. 1. Ventral view.
Fig. 2. Plates of the epicone showing plate overlap directions (arrowheads).
Fig. 3. Plates of the hypocone showing plate overlap directions (arrowheads). Dashed line indicates position and maximum extent of antapical flanges (lists).

likely, however, that for practical reasons, palynologists will continue to use nomenclature based on fossil-based taxa and so for clarity we include a list (Table 1) of the dual nomenclature for the taxa studied. Plate and tabulation notations follow the homologue approach for the gonyaulacalean standard tabulation proposed by Fensome *et al.* (1993), which involves four apical plates, six precingular plates, six postcingular plates, one left ventral posterior intercalary plate, and one antapical plate.

For each species, important references, including illustrations, are quoted.

Cyst–theca relationships

Gonyaulax elongata (Reid) Ellegaard, Daugbjerg, Rochon, J. Lewis & I. Harding *comb. nov.*

Figs 1–30

BASIONYM: *Spiniferites elongatus* Reid (1974, pp. 602–604, figs 23, 24).

SYNONYMS: *Gonyaulax* sp. 1 in Wall & Dale (1968, pl. 1, fig. 16); *Hystrichosphaera* sp. A in Harland & Downie (1969, pl. 7, fig. 4).

OTHER REFERENCES (as *S. elongatus*): Reid (1974, figs 23, 24); Dale (1976, pl. 1, fig. 8); Harland *et al.* (1980, fig. 2K, L); Harland (1982a, pl. 1, figs 9, 10); Dale (1983, figs 7, 8); Harland (1983, pl. 44, figs 7, 8); Harland & Sharp (1986, pl. 1, figs 1–8 and pl. 2, fig. 9); Matsuoka (1987, pl. 1, figs 9, 10); Matsuoka (1992, pl. 1, fig. 6); Nehring (1997, fig. 7); Rochon *et al.* (1999, pl. 6, figs 7–10).

MOTILE CELL: Size, 32–41 × 28–34 μm ($n = 25$, $\bar{x} = 36 × 30$ μm), with tabulation formula 2 pr, 4′, 6″, 6c, ≥ 4s, 6‴, 1p, 1⁗ (Figs 1–3).

The motile stage has a conical epicone with slight shoulders and a short apical horn (Figs 4, 5, 17). The hypocone is conical with a flat antapex (Figs 5, 16) and the cell is almost circular in polar view (Fig. 12). Because of a triangular antapical flange, the cell often appears diamond-shaped in ventral or dorsal view (Figs 9, 17). The cells are brown and have typical S-type gonyaulacalean tabulation. The plates are often heavily ornamented with a reticulate pattern (Fig. 8), sometimes also present on the cingulum (Fig. 7), sulcus and flanges (Fig. 8). However, the degree of ornamentation varies greatly and newly divided cells have no ornamentation on the recently formed plates (Fig. 16). There are only a few pores on the plates (Fig. 10), mostly on the cingular margins (Figs 8, 11). The plate boundaries are often difficult to discern (Figs 4, 11) and the plates are difficult to distinguish under the microscope. The Q plate ['c vorne' in Taylor–Evitt terminology (Fensome *et al.* 1993)] is small (Fig. 13) and often difficult to distinguish from the third apical plate (Figs 5, 7). On most specimens, the fourth apical plate is very difficult to separate from the Q and the first apical plates (Fig. 7). The ventral pore is clear only on some specimens (Fig. 4). The apical pore area is surrounded by a smooth ridge formed by the edges of the surrounding plates (Fig. 6). The third precingular plate is broad and overlaps all the adjoining plates (keystone plate; Fig. 9), and the second and third apical plates meet mid-dorsally (Fig. 17). The sixth precingular and second postcingular plates are elongated triangles (Figs 5–7); the first postcingular plate is rectangular and small (Fig. 8).

The cingulum is wide (2.5–3.5 μm) and deep, with the ends of the cingulum forming an angle of 16–33° with the main axis of the cell and a displacement of 2–3 cingular widths (Figs 4, 6–7). There are flanges (lists) on the cingular margin (Figs 6, 8, 9). The sulcus widens broadly towards the antapex (Figs 15, 16) and is deeply excavated (Fig. 12), with the sulcal depression ending near the upper cingular rim (Fig. 6). The antapical intercalary plate only just touches the antapical plate (Figs 8, 10). There are flanges on the antapical intercalary
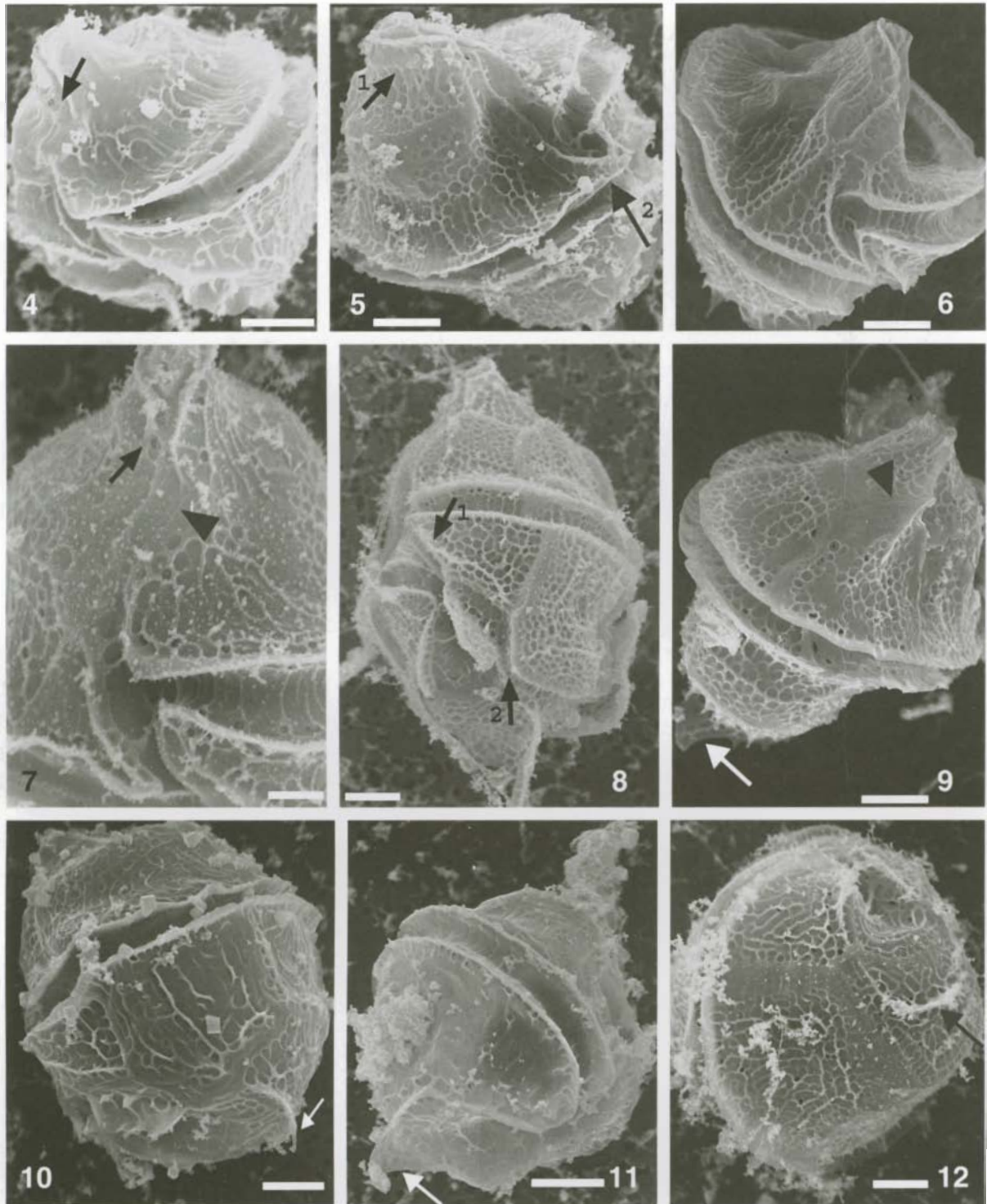
Figs 4–12. Motile cells of *Gonyaulax elongata* from culture, SEM. Scale bars = 5 μm or 2.5 μm (Fig. 7).
   Fig. 4. Ventral–left view, showing the ventral pore (arrow).
   Fig. 5. Ventral–right view, showing the Q plate (arrow 1) and the triangular sixth precingular plate (arrow 2).
   Fig. 6. Ventral view, showing the course of the cingulum, the upper part of the sulcus and the triangular sixth precingular plate.
   Fig. 7. Ventral view, showing the Q plate (arrow), the first apical plate (arrowhead) and the upper part of the sulcus.
   Fig. 8. Left–antapical view, showing the first postcingular plate (arrow 1), the boundary between the posterior intercalary plate and the antapical plate (arrow 2) and heavily ornamented plates.
   Fig. 9. Dorsal view, showing the shape of the cell, the antapical flange (white arrow), the mid-dorsal keystone plate (black arrowhead) and the flanges on the cingulum.
   Fig. 10. Antapical–left view, showing plates with poorly developed ornamentation and the position of the antapical flange (arrow).
   Fig. 11. Right view, showing the lower part of the sulcus and the antapical flange (arrow).
   Fig. 12. Antapical view, showing plates of the hypocone, the shape of the cell and the flange (arrow).

(Fig. 8), the sixth postcingular (Fig. 8) and the antapical plates (Figs 8, 9, 11, 17), and there are 0–8 small spines on the antapical plate (Figs 6, 9). All flanges and spines are variably developed and sometimes absent. The boundaries of the sulcal plates are clear in the antapical part of the sulcus (Figs 15, 16), but obscured in the anterior end. The posterior sulcal plate (ps) is broad and relatively short (Figs 15, 16) and the boundary between the left (ls) and right (rs) sulcal plates originates from the middle of the anterior boundary of the ps plate. The anterior part of the sulcus is narrow (Figs 6, 7, 14), with a hook-shaped anterior sulcal plate (as; Fig. 14).

The plate overlap pattern (Figs 2–3) is as described for *G. digitalis* (Lewis *et al.* 2001). The triangular flange on the antapical plate and the diamond shape of the cell in dorso-ventral view are characteristic features of this species, although the flange is often small (Figs 10, 12): it is sometimes visible under LM (Fig. 17) and sometimes not (Figs 13, 16).

CYST: Size, 35–62 × 20–32 μm ($n = 19$, $\bar{x} = 41 × 27$ μm), with paratabulation formula 4′, 6″, 6c, ?s, 1p, 6′′′′, 1′′′′ (Figs 20–22); archeopyle at 3″.

The cyst is rounded and elongate in lateral view (Figs 18, 19, 23–25) and circular in polar view (Fig. 26). The periphragm (the outer layer of the wall) is thin and slightly coarse (Figs 23, 27); the endophragm (the inner layer of the wall) is smooth and about 0.3 μm thick (Fig. 28). An apical protuberance was not seen. The processes are gonal (i.e. they lie at the intersection between the paraplates: Williams *et al.* 2000) and of variable length, from an average of 2 μm (Fig. 25) to 8 μm (Fig. 27) ($n = 5$, 4–8 processes measured per cyst). The antapical processes are typically the longest (6–12 μm, $n = 11$) and the processes at the paracingulum are the shortest (0–7 μm, $n = 11$), except for cysts with reduced processes, where all are of about equal length (Figs 25, 29). Fully developed processes are trifurcate with bifid endings (Figs 23, 27), whereas reduced processes may taper to a point, end bluntly, or end with a slight fork (Fig. 25). Membranes along the parasutures define the paraplates. These membranes can be feebly (Figs 19, 25, 29) to well developed (Figs 26, 27), and are seen most often at the antapex, but sometimes cover the entire cyst body (Fig. 30). The extension of membranes onto paraplates often makes the latter appear rounded (Figs 23–25).

The paracingulum is displaced by about two cingular widths, with no overlap (Figs 23, 29). The parasulcus is triangular, widening towards the antapex (Fig. 23). Only the posterior sulcal plate (ps), anterior sulcal plate (as) and right sulcal plate (rs) are visible (Figs 23, 29). In SEM, the preformed archaeopyle is often visible (Figs 24, 28).

Wild cysts were classified into three groups on the basis of spine length and degree of membrane development: (1) cysts with long or normal processes (Figs 27, 28); (2) cysts with reduced processes (Fig. 29); and (3) cysts resembling the cyst-based taxon *S. frigidus* Harland & Reid (Fig. 30). *Spiniferites frigidus* was described from arctic Canada as a very membranous elongate *Spiniferites* (Harland *et al.* 1980). A fourth cyst form, described from the Norwegian Sea as '*Spiniferites* cf. *S. elongatus*' (Harland & Sharp 1986) was not recognized in our study. Type 1 was isolated from material from all six locations, type 2 from material from the Orkneys, Canada (comprising almost half of the isolated specimens), Greenland
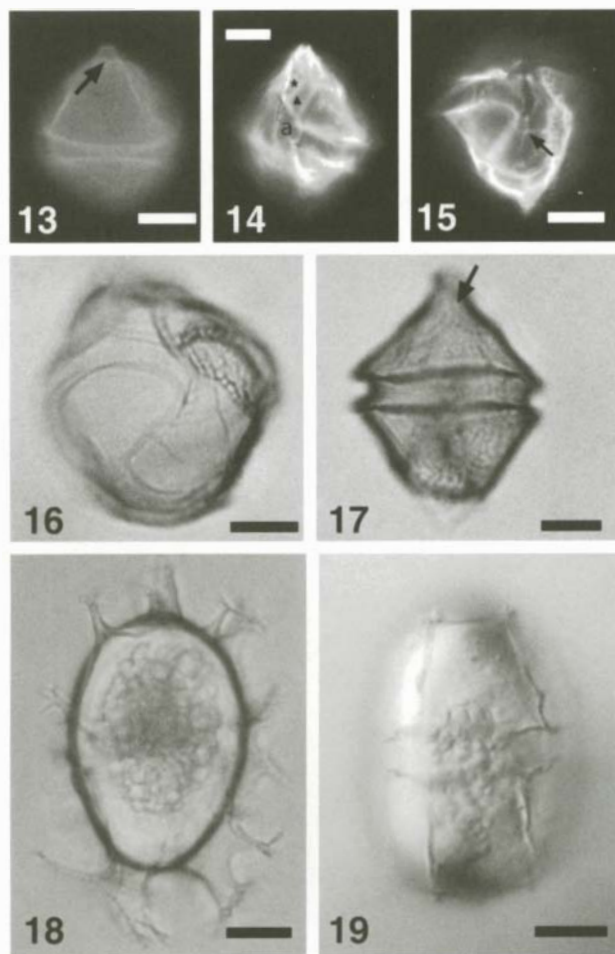
Figs 13–19. *Gonyaulax elongata* from culture, LM. In Figs 13–15, the thecal plates are stained with calcofluor white and viewed under UV illumination; Figs 16–18 used bright field optics and Fig. 19 Nomarski differential interference contrast. Scale bars = 10 μm.
Figs 13–17. Motile cells.
Fig. 13. Left view, showing the boundary of the third apical plate and the Q plate (arrow).
Fig. 14. Ventral view, showing the first (▲) and fourth (*) apical plates and the anterior sulcal plate (a).
Fig. 15. View of the sulcus, showing the boundaries between the posterior, left and right sulcal plates (arrow).
Fig. 16. Right–antapical view, showing newly formed plates to the right of the sulcus.
Fig. 17. Dorsal view, showing the overall shape of the cell and the boundary of plates 2′ and 3′ (arrow).
**Figs 18, 19.** Cysts.
Fig. 18. Lateral view (optical section), showing well-developed processes.
Fig. 19. Lateral surface view, showing reduced processes.

and the North Sea, and type 3 only from Canadian material. Likewise, in cysts produced in culture, type 1 (Figs 18, 23–24) was found in strains from all three locations, type 2 (Figs 19, 25) in Orkney and North Sea strains, and type 3 (Fig. 26) only in Canadian strains (Table 2).

In summary, it is possible to distinguish the motile cells of *G. elongata* from those of other *Gonyaulax* species by the triangular antapical flange, the nearly conical epicone, the reticulation of the sulcus, and the narrow anterior sulcal plate. The tabulation pattern is often difficult to discern.
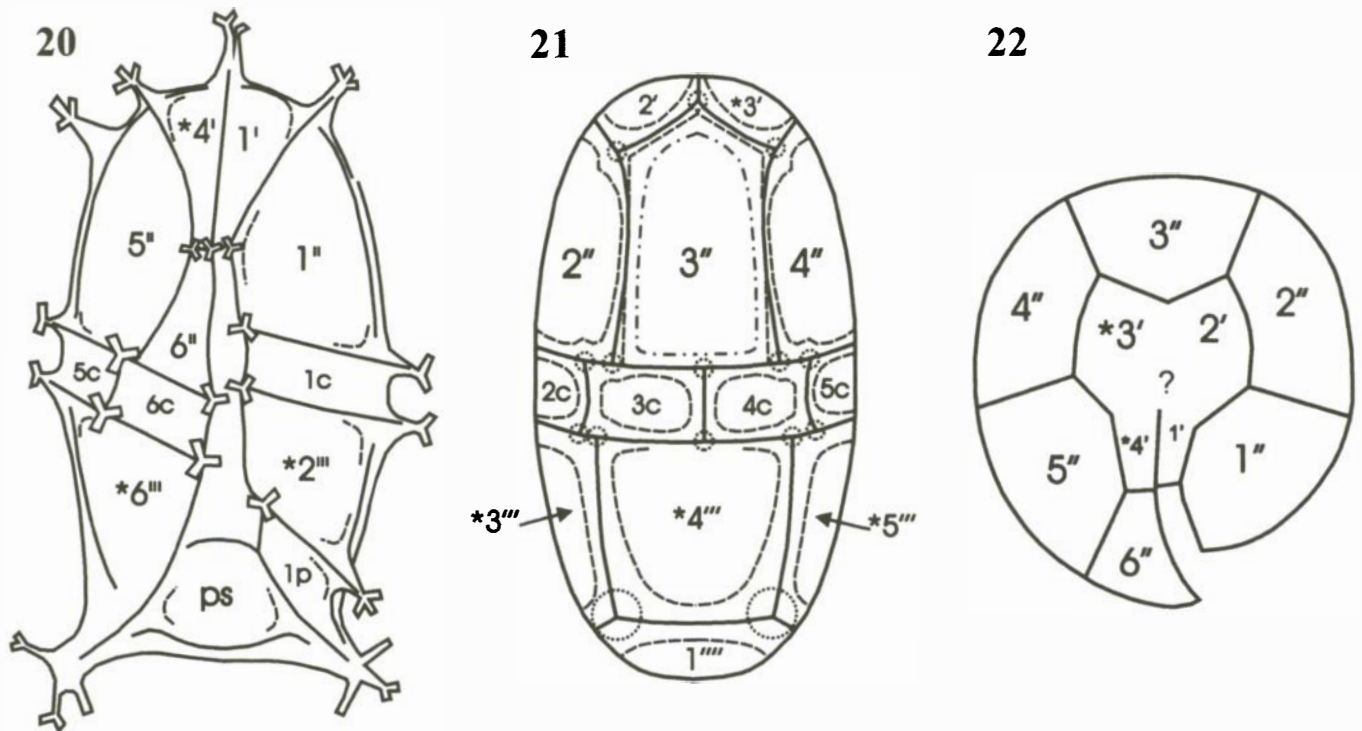
Figs 20–22. *Gonyaulax elongata*: line drawings of the tabulation pattern of the cyst.
Fig. 20. Ventral view showing position and relative development of process terminations.
Fig. 21. Dorsal view. Dashed lines indicate the extent of suturocavation, dotted circles show the position and relative sizes of the processes, and the dashed and dotted lines show the position of the preformed, reduced archaeopyle.
Fig. 22. Apical view.

Gonyaulax membranacea (Rossignol) Ellegaard, Daugbjerg, Rochon, J. Lewis & I. Harding *comb. nov.*

Figs 31–45

BASIONYM: *Hystrichosphaera furcata* var. *membranacea* Rossignol (1964, p. 86, pl. 1, figs 4, 9, 10; pl. 3, figs 7, 12).

SYNONYM: *Spiniferites membranaceus* (Rossignol) Sarjeant

OTHER REFERENCES (as *S. membranaceus*): Reid (1974, pl. 3, figs 28–31); Harland (1983, pl. 45, figs 3, 4); Lewis *et al.* (1999, figs 1–19); Rochon *et al.* (1999, pl. 8, figs 5–9).

The cyst–theca relationship of *G. membranacea* has been described in detail by Lewis *et al.* (1999, as *S. membranaceus*). The strain described below (strain UW398) differs from this description in some aspects, which initially led us to consider it a separate species. We include the description of this strain to illustrate the large morphological intraspecific variation possible in *Spiniferites–Gonyaulax*.

MOTILE CELL: Size, 31–37 × 25–30 μm (*n* = 40, $\bar{x}$ = 34 × 28 μm).

The overall shape (Figs 31, 40), size and colour are as described previously (Lewis *et al.* 1999). The thecal plates differ in being difficult to distinguish and in having little reticulate ornamentation. Instead, the plates have very conspicuous circular depressions, each surrounded by a rim, and sometimes with a pore in the centre (Figs 31, 32). The cingulum and sulcus are as described previously. The cells usually have two spines on the posterior sulcal rim, 2–4 μm in length (Figs 31, 40), one of which is often more prominent (Fig. 32). The lack

of reticulate ornamentation and the prominent circular depressions are the main features of this strain, distinguishing it from motile cells of other stains of *G. membranacea* (Lewis *et al.* 1999). However, some specimens of the same strains studied by Lewis *et al.* (1999), show a tendency to similarly reduced reticulation (Figs 37, 38; strain UW345).

CYST: Although the cyst isolated was identified as '*Spiniferites membranaceus*', cysts formed in culture in this strain differed so much from other cysts produced by this species that they would be very unlikely to have been recognized as *G. membranacea* and could even, on the basis of morphology, have been considered to belong to a cyst genus other than *Spiniferites*.

Cysts of strain UW398 are 28–35 μm in diameter (*n* = 10, $\bar{x}$ = 32 μm). The cyst body is subspherical (Figs 33, 43–45) to spherical (Fig. 36) with a smooth endophragm (Figs 34–36); it sometimes displays a preformed archaeopyle (Figs 33, 35), but otherwise featureless. The periphragm is very thin and perforate (Figs 34, 36) and in places displays a marked separation from the endophragm, often as suturocavation (Fig. 42); in extreme examples, the periphragm separates completely from the inner wall layer (Figs 34, 41, 44). On some specimens, the periphragm is only partially developed (Figs 35, 36). In specimens with relatively little separation between the wall layers, partial paratabulation is often evidenced by marked suturocavation (*sensu* Williams *et al.* 2000) (Figs 33, 36). A paracingulum can be seen on a few specimens (Figs 33, 42), but the fragile nature of the periphragm makes it very difficult to determine a tabulation scheme for the cysts. Pro-
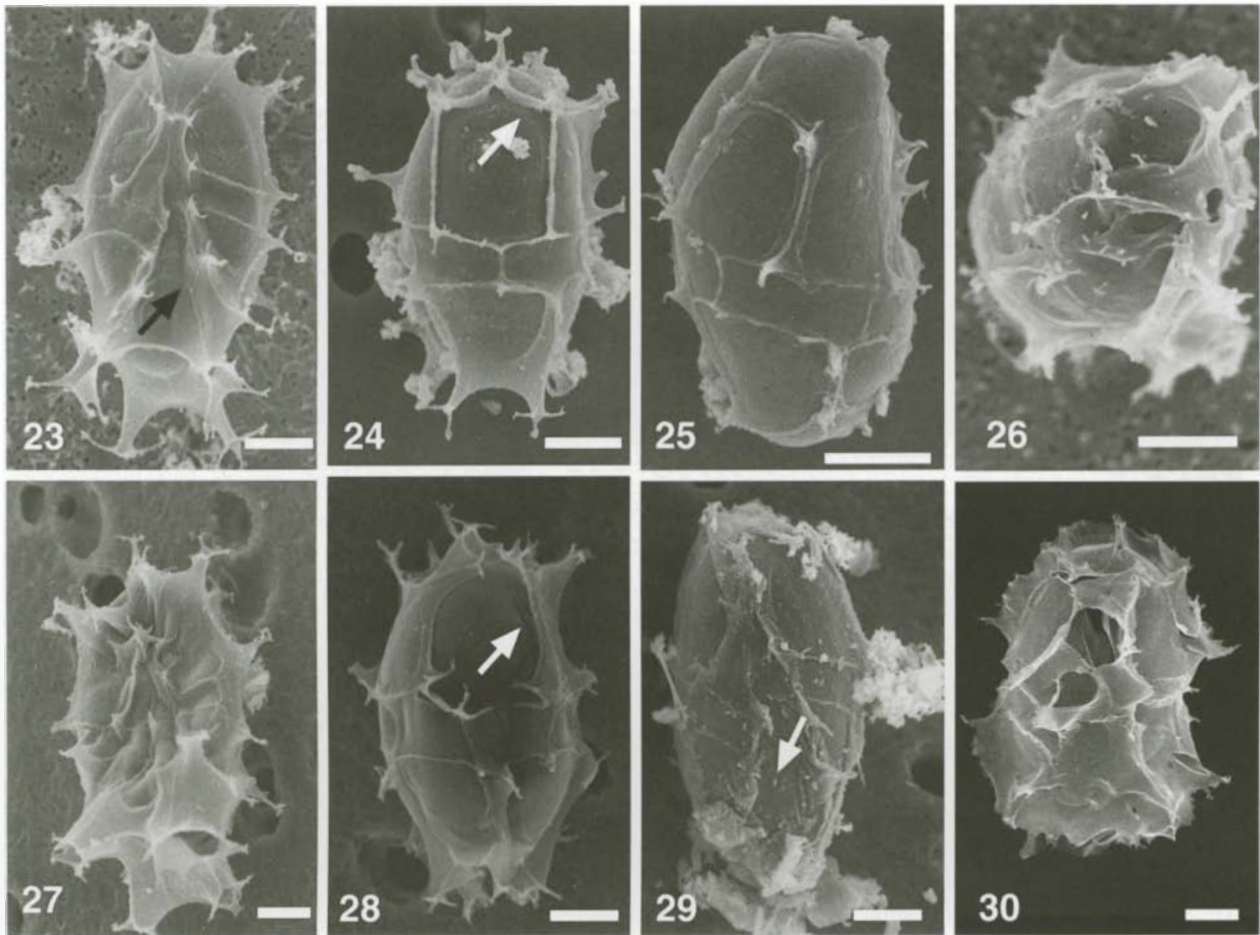
Figs 23–30. *Gonyaulax elongata* cysts, SEM. The upper row of micrographs (Figs 23–26) shows four cysts formed in culture, with varying development of processes and membranes. The lower row (Figs 27–30) shows four wild cysts, with varying development of processes and membranes, each placed under a corresponding cultured cyst. Scale bars = 10 μm.

Fig. 23. Ventral view of cyst with well-developed processes, showing the cingulum–sulcus area and a sulcal parasuture (arrow).

Fig. 24. Dorsal view of cyst with normal processes, showing the preformed archaeopyle (arrow shows suture).

Fig. 25. Right view of cyst with very reduced processes.

Fig. 26. Polar view of cyst with extensive membranous development (from a Bedford Basin strain).

Fig. 27. Ventral view of a wild cyst from Bedford Basin with well-developed processes.

Fig. 28. Dorsal view of a wild cyst from Greenland with normal processes, showing the archaeopyle suture (arrow).

Fig. 29. Ventral view of a wild cyst with reduced processes from Bedford Basin showing a sulcal parasuture (arrow).

Fig. 30. Lateral view of a wild cyst from Bedford Basin with extensive membranous development.

cesses are sometimes visible (Fig. 44) and sometimes not (Fig. 34). Some specimens have a slight apical boss (Fig. 45). The most conspicuous feature of the cyst is the very thin, suturocavate, ballooning periphragm, which is quite distinct even under low magnification in LM (Fig. 41). The periphragm often collapses during preparation for SEM (Figs 34, 35). Although the ballooning periphragm has not previously been described for *G. membranacea* cysts, some specimens from other strains, studied by Lewis *et al.* (1999), show similar perforations in the periphragm (Fig. 39; strain UW334). Some specimens from strain UW398 display the antapical suturocavate process typical for *G. membranacea* (Fig. 43).

DIFFERENCES FROM OTHER *GONYAULAX* SPECIES: The motile cells of *G. membranacea* are distinguished from those of other *Gonyaulax* species by the lack of reticulation on the plate margins or on the entire plate, the 2–4 thin spines, where one is often more prominent, and the narrow ps plate.

rDNA sequence and phylogeny

Phylogenetic analyses based on partial LSU rDNA sequences show that the *Gonyaulax* group is monophyletic, with 100% bootstrap support in both MP and ML analyses (Fig. 46). The other *Gonyaulax* species included in the analyses, in addition to *G. elongata* and *G. membranacea* strain UW398, are illustrated in Figs 47–54. The topology within the *Gonyaulax* clade is generally well supported in terms of bootstrap values, whereas the topology for the three species of *Alexandrium* and some higher levels received low bootstrap support. Because of the relatively low bootstrap values, these analyses do not indicate clearly which genus is the closest sister taxon to the
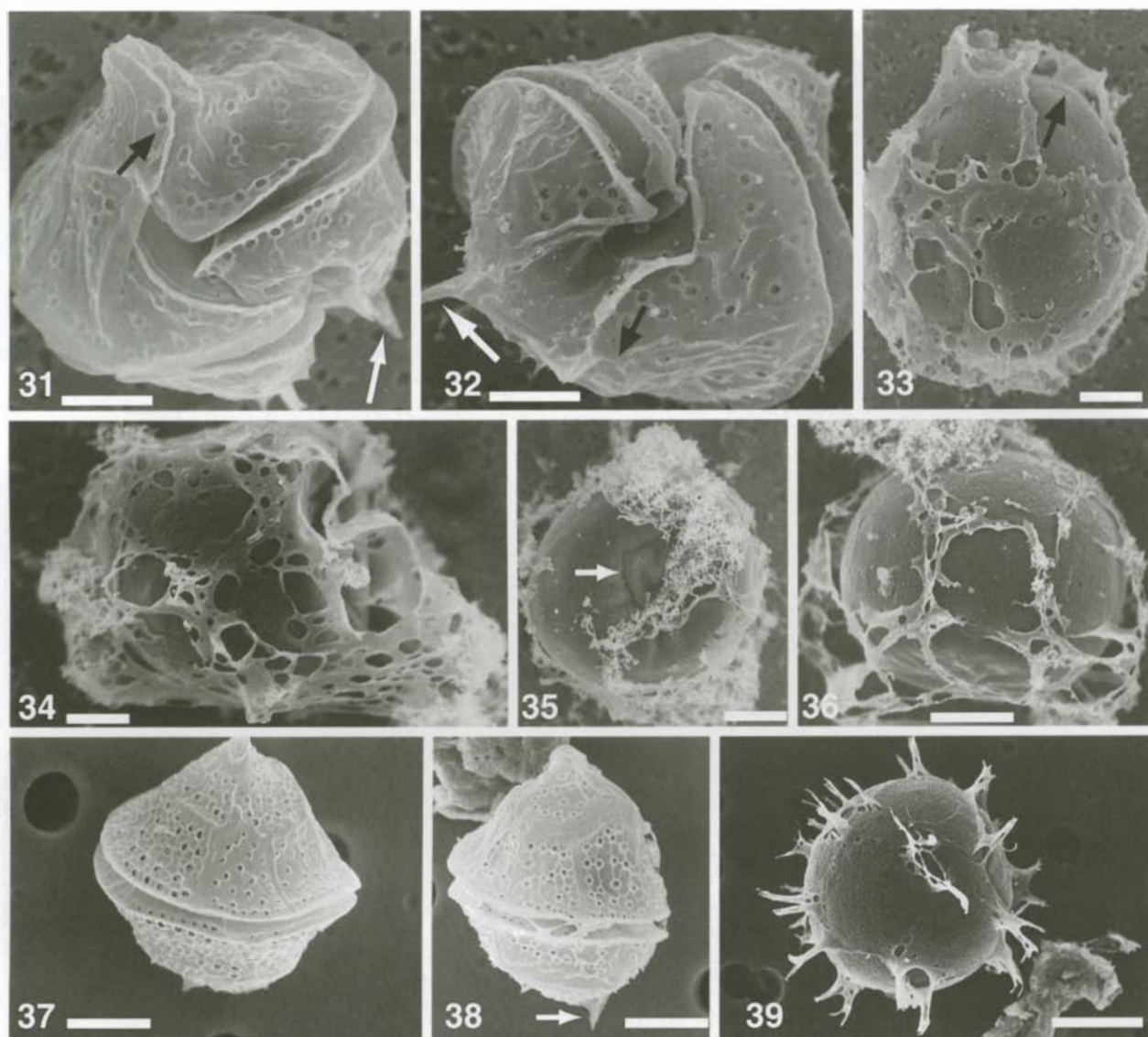
Figs 31–39. SEM micrographs of *Gonyaulax membranacea*. Figs 31–32 show motile cells and Figs 33–36 show cysts from strain UW398. Figs 37–38 show motile cells from strain UW345 and Fig. 39 shows a cyst from strain UW334. Scale bars = 5 μm (Figs 31–34) or 10 μm (Figs 35–39).

Fig. 31. Ventral view showing the ventral pore (black arrow), the plate ornamentation, the cingulum–sulcus area, and antapical spines (white arrow).

Fig. 32. Ventral–antapical view showing the sulcus, one well-developed spine (white arrow), and the boundary between the antapical intercalary plate and the antapical plate (black arrow).

Fig. 33. Cyst with clear suturocavate paratabulation, particularly in the paracingulum, and showing the archaeopyle suture (arrow).

Fig. 34. Cyst with very perforate periphragm.

Fig. 35. Cyst with preformed archaeopyle (arrow).

Fig. 36. Cyst with partial periphragm attached in penitabular areas.

Fig. 37. 'Normal' motile cell with poorly developed reticulation.

Fig. 38. 'Normal' motile cell with one well-developed antapical spine (arrow).

Fig. 39. 'Normal' cyst with perforation in the periphragm.

Gonyaulax–Spiniferites cluster. As expected from cyst morphology, *G. membranacea* (Fig. 51) and *G.* cf. *spinifera* (Fig. 53) are closely related. Considering its *Bitectatodinium*-type cyst morphology (Fig. 54), it is surprising that *G. digitalis* (*B. tepikiense*) appears within the *Gonyaulax–Spiniferites* group, rather than as sister group to the species with *Spiniferites* cysts. Also surprisingly, *G. baltica* forms a sister taxon to the rest of the group, although both its cyst (Fig. 52) and motile cell (Fig. 48) morphology are similar to those of *G.* cf. *spinifera* and *G. membranacea*. Strain K-0487 from the Scandinavian Culture Centre of Algae and Protozoa was originally described as *G. spinifera* and is identical to *G. baltica* in this study. The sequence divergence between species within the *Gonyaulax–Spiniferites* group (12–23%) is comparable with
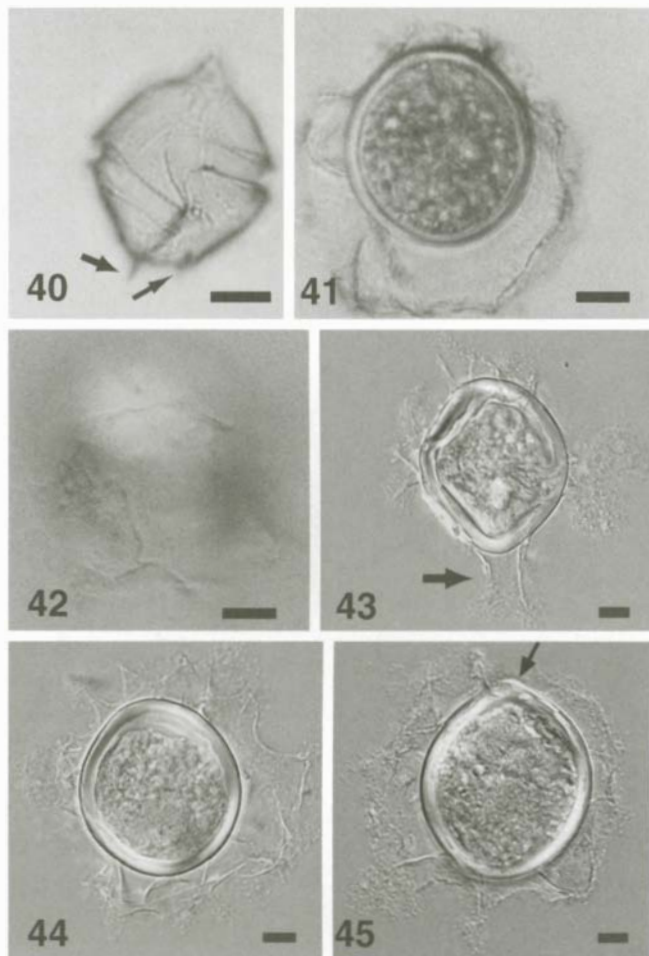
Figs 40–45. *Gonyaulax membranacea*, strain UW398: a motile cell (Fig. 40) and cysts (Figs 41–45), LM, in bright field (Figs 40, 41) or Nomarski differential interference contrast (Fig. 42). In Figs 43–45, automontage methods have been used to convert an image stack into a single 2D image (see text). Scale bars = 10 μm (scale only approximate for Fig. 45).

Fig. 40. Ventral view, showing the overall shape of the cell and the antapical spines (arrows).
Fig. 41. Lateral view of cyst with well-developed cavation.
Fig. 42. Surface view of parasutures on the periphragm.
Fig. 43. Cyst with suturocavate parasutures and an antapical suturocavate process (arrow).
Fig. 44. Cyst with well-developed cavation and suturocavate parasutures.
Fig. 45. Cyst with an apical boss (arrow).

Fig. 46. Phylogeny of the Gonyaulacales, with emphasis on *Gonyaulax*, inferred from partial LSU rDNA sequence data. The topology was inferred from ML analysis, using 10 random additions of sequences and the F84-model with empirical base frequencies in PAUP* (ver. 4b8). The best ln-likelihood score was −8403.285. LSU rDNA sequences from *H. triquetra* and *Prorocentrum micans* were used to root the tree. The branch lengths are proportional to the number of substitutions per site. Bootstrap values are provided to the left of internal nodes: numbers from ML analyses (100 replicates) are shown above and numbers from unweighted MP analyses (1000 replicates) below. Only bootstrap values above 50% are shown. Unweighted parsimony analyses with 1000 random additions of sequences in heuristic searches produced three equally parsimonious trees, each of 1483 steps (trees not shown: CI = 0.604, RI = 0.664).

that between the three species of *Alexandrium* Halim (16–20%) and higher than that between the three species of *Ceratium* Schrank (7–11%).

DISCUSSION

Life cycle and growth

Gonyaulax elongata and *G. membranacea* grew slowly in culture, encysted quickly and spontaneously, and the cultures were short lived. It was therefore not possible to test whether there is a connection between morphological variation in the cysts and ecological factors, like that present in *G. baltica* (Ellegaard *et al.* 2002) and *Lingulodinium polyedrum* (F. Stein) Dodge (Hallett 1999). *Gonyaulax digitalis* (Lewis *et al.*
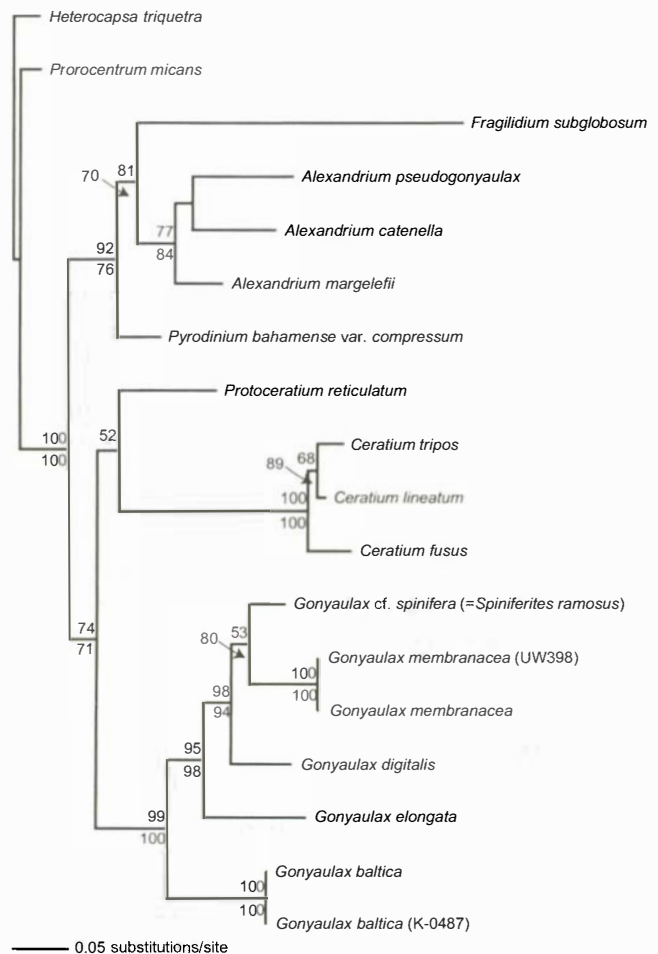
2001) and some strains of *Protoceratium reticulatum* (unpublished data) also encyst quickly and spontaneously in culture and *G. digitalis* also grows slowly and dies quickly (Lewis *et al.* 2001). *Protoceratium reticulatum* has previously been reported to be over-represented in the cyst flora, relative to its representation in the plankton (Dale 1976). Perhaps it is a widespread strategy for some cyst-forming species to exist only for short periods in the motile stage, encyst rapidly, and spend most of their time in the cyst stage.

Cyst–theca relationships

GONYAULAX ELONGATA: The cyst of *G. elongata* is easily recognizable and has been described thoroughly (e.g. Reid 1974; Harland & Sharp 1986). It has been found in many studies of
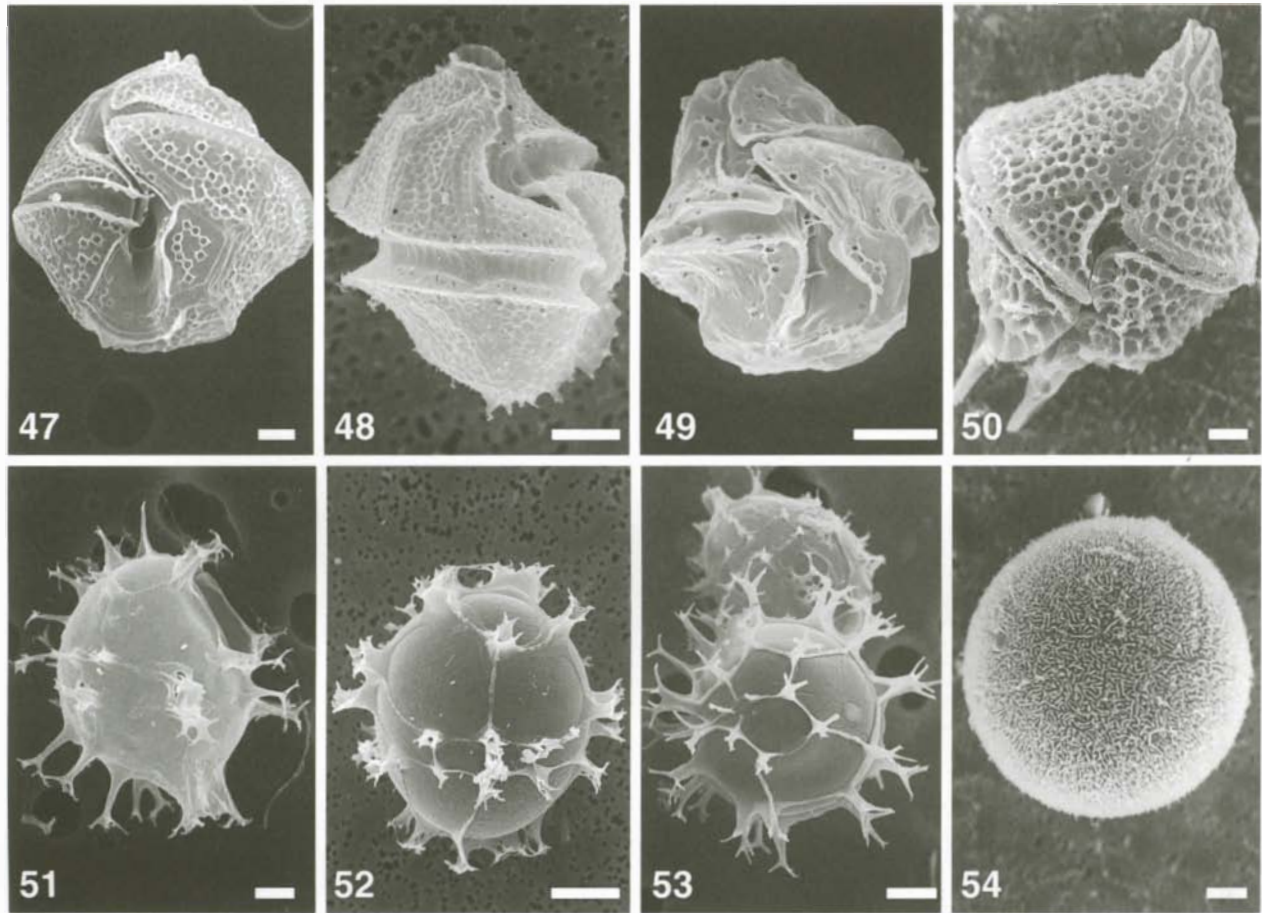
Figs 47–54. Motile cells (Figs 47–50) and cysts (Figs 51–54) of the other *Gonyaulax* species included in the phylogenetic analyses, SEM. Scale bars = 5 μm or 10 μm (Fig. 52).
  Figs 47, 51. *G. membranacea,* with *Spiniferites*-type cyst.
  Figs 48, 52. *G. baltica,* with *Spiniferites*-type cyst.
  Figs 49, 53. *G.* cf. *spinifera,* with *Spiniferites*-type cyst.
  Figs 50, 54. *G. digitalis,* with *Bitectatodinium*-type cyst.

cysts in Recent sediments, primarily in polar and subpolar regions (e.g. Wall *et al.* 1977; Dale 1996; Rochon *et al.* 1999). The cysts observed in this study fit the original description of *S. elongatus,* except that Reid (1974) could not see any sulcal paraplates. Also, in the original description, the shortest process was 5 μm in length, whereas processes down to 1 μm (and an average of 2 μm on cysts with reduced processes) were recorded in the present study. On many cysts, processes could not be seen in LM, so that the cysts resembled elongate *Impagidinium* cysts rather than *Spiniferites*.

Harland *et al.* (1980) discussed whether *S. frigidus* was a separate species or a morphotype of *G. elongata.* The fact that in the present study *S.* cf. *frigidus*-type cysts were primarily found in Bedford Basin sediment samples points to the possibility that the Bedford Basin population is different from those of the other sampling sites. Unfortunately, this could not be verified, because only one strain was established from Bedford Basin: it was short lived and did not produce many cysts or motile cells. Therefore, it was not possible to test whether *S. frigidus* is a separate species or a morphotype of *S. elongatus.*

Links between *S. elongatus–S. frigidus* and *G. spinifera,* the *G. spinifera* group and '*Gonyaulax* sp. Indet.' have been re-

ported or inferred many times (see references in Head 1996). In most of these studies, however, the cysts were not germinated and the link was supported only by reference to other studies. The only study in which a presumed *S. elongatus* cyst was actually germinated was that of Wall & Dale (1968), who germinated an elongate *Spiniferites* cyst that they named *Gonyaulax* sp. 1 and described as being similar to *Pterospermum ovum* Gaarder. In 1974, when Reid formally described *S. elongatus,* he listed *Gonyaulax* sp. 1 of Wall & Dale (1968) as a synonym, although he thought *P. ovum* was synonymous with *S. belerius* Reid. Wall & Dale (1968) described the motile cell of *Gonyaulax* sp. 1 as small, green and resembling that of *G. scrippsiae* Kofoid in shape and size. Later, Dale (1976) reported the motile stage of *S. elongatus* as belonging to an undifferentiated *G. spinifera* group, which he defined as comprising *G. spinifera, G. digitalis* and *G. scrippsiae.* Neither Wall & Dale (1968) nor Dale (1976) illustrated the motile cell of *Gonyaulax* sp. 1. *Gonyaulax elongata* cysts from the Kieler Bight have subsequently been germinated (Nehring 1997, as *S. elongatus*), but with no illustrations or descriptions of the motile stage.

The description of the motile stage of *G. elongata* as presented in this study does not fit any previous descriptions of

Table 4. Comparison of motile cells of the *Gonyaulax* species examined in this study, and Kofoid's description of *G. spinifera*. ± = may be present or absent.

	G. spinifera[1]	*G. elongata*	*G. membranacea*, UW398	*G. membranacea*[2]	*G. baltica*[3]	*G.* cf. *spinifera*[2]	*G. digitalis*[4]
Figures	—	4–17	31–32, 40	37–38, 47	48	49	50
Length (μm)	24–50	32–41	31–37	30–48	31–37	22–43	40–63
Width (μm)	20–37	28–34	25–30	23–40	27–32	17–43	26–43
Shoulders		slight, diamond shaped	intermediate	intermediate	slight	slight	pronounced
Reticulation	smooth to faint	weak to pronounced	weak	pronounced, smooth, plate margins	pronounced	weak	pronounced
Pores		few	intermediate	intermediate to many	few to many	few to intermediate	many
Ring		yes	yes, conspicuous	±	±	±	no
Cingulum							
Reticulation		±	no	±	±	±	yes
Width (μm)	3–7	2.5–3.5	2–3	2.5–3.5	3–4	2.5	3–4
Displacement[5]	2.3–3	2–3	2–3	2.5–4	2.5–4.5	1.5–2	2
Overhang[5]	1.5–2	1.8–2.5	2–3.5	2–4	2–3.3	1–1.5	~1
Angle (°)	27–40	16–33	22–38	20–29	23–45	27–29	~0–15
Sulcus							
Reticulation		yes	no	no	no	no	no
Widening	yes	yes	slight	slight	no	slight	yes
Anterior part of sa	widening	narrow	widening	slightly widening	broad	slightly widening	narrow
Q	not separated	separated, small	separated	separated	separated, small	not separated	separated, small
Antapical spines	0–2	1 flange, 0–8 small	1–2, one often prominent	1–4, one often prominent	0–10	0–4	2–3
Ornamentation	small	triangular flange	fine, long	±finned	small, ±finned	usually small	long, finned

[1] Kofoid (1911).
[2] Lewis *et al.* (1999).
[3] Ellegaard *et al.* (2002).
[4] Lewis *et al.* (2001).
[5] measured in cingulum widths.

Gonyaulax species. However, there are over 50 species of *Gonyaulax* known and many are described or illustrated poorly. The characteristic triangular antapical flange is similar to those depicted on drawings of *G. monacantha* Pavilliard and *G. jolliffei* Murray & Whitting. However, *G. monacantha* has a conspicuously different ornamentation, *G. jolliffei* has a long apical horn, and both are substantially larger than the motile cell of *G. elongata*. A line drawing of *G. manginii* Fauré-Fremiet (Fauré-Fremiet 1908, fig. 16) has a single triangular spine similar to the antapical flange of *G. elongata,* but an illustration of the species (Fauré-Fremiet 1908, pl. 16, fig. 19) shows a specimen with thecal reticulation more similar to that of *Protoceratium reticulatum.*

GONYAULAX MEMBRANACEA: The variability in the motile stages of *Gonyaulax* species (Lewis *et al.* 1999; Ellegaard *et al.* 2002; this study) may explain some of the confusion in the literature about their identities. Many early reports on the motile stages germinated from *Spiniferites* cysts are based on just a few cells, which may have lacked features that characterize individual species. An example is the triangular flange, which makes *G. elongata* easy to recognize and distinguish from *G. spinifera*. The intraspecific variation in both the cyst and motile stage is broad in the case of *G. membranacea,* and strain UW398 differs from previous descriptions of the motile stage of *G. membranacea* (Lewis *et al.* 1999) in the lack of reticulate ornamentation. It differs from previous descriptions of the cyst of *G. membranacea* (Lewis *et al.* 1999 and references therein) in size (28–35 µm vs 41–54 × 37–50 µm) and the ballooning periphragm, and because of these morphological characters, it was originally thought to be a new species. However, the LSU rDNA sequence shows that it differs from *G. membranacea* in only 1 bp (out of 1119). On the basis of the morphological similarities in cyst and mobile stages discussed in the Results section, and the LSU rDNA data, we choose to assign this strain to *G. membranacea,* in spite of the differences in cyst morphology. We include the description of strain UW398 here as an example of the large morphological variation possible within cysts of the *Spiniferites* group of *Gonyaulax*. A similar case of lack of agreement between morphological and LSU rDNA data is found in the *A. tamarense* complex, where an analysis has shown that strain genotypes group according to geography rather than morphology (Scholin *et al.* 1995). Lewis *et al.* (1999) described the motile stage of *G. membranacea* in detail for the first time and considered it to be close to *G. diegensis,* with differences in size, girdle overhang and the shape of the sixth precingular plate, but they did not assign a name to the motile stage. In Kofoid's (1911) account, the specimen of *G. spinifera* shown in pl. 10, figs 9, 10, is different from that in pl. 16, fig. 39. The former specimen has a triangular sixth precingular plate that is not very elongate, as well as two prominent spines, whereas the latter has a more elongate sixth precingular plate and four fine, short spines. These two specimens could be separate species, the former possibly being a specimen of *G. membranacea.*

There are larger differences between *Gonyaulax* species in cyst morphology than in motile cell morphology (Lewis *et al.* 1999, 2001; Ellegaard *et al.* 2003). This has been one of the causes of the 'Spiniferites enigma', where cysts from six cyst-based genera apparently germinated to give motile cells belonging to a single species complex, according to the motile

cell–based taxonomy (Dale 1983). The conservative nature of motile cell morphology vs cyst morphology is also true in other dinoflagellate genera. Dale (1978) pointed out that large differences in cyst morphology can correspond to only minor differences in thecae. The genus *Protoperidinium* Bergh displays a similar confusion in cyst forms among the more stable motile thecate patterns (Harland 1982b) and, in the genus *Scrippsiella* Balech, individual species are more easily distinguished on the basis of their cyst stage than on their motile stage (Lewis 1991). The same pattern is seen within species: the variability in cyst morphology is often more striking than the variability within the motile stage and can sometimes be correlated with environmental variation (e.g. in *G. baltica*: Ellegaard *et al.* 2002)

LSU rDNA sequences, phylogeny and nomenclature

Recent work has determined that subtle morphological differences between motile cells within *Gonyaulax* may have taxonomic significance, allowing species separation. LSU rDNA sequence data confirm this, and the sequence divergence between species seems to accord with the differences in cyst morphology rather than the more subtle differences in motile cell morphology (Table 4). However, the LSU rDNA data raise questions about the phylogenetic validity of some of the cyst-based genera, because *G. digitalis–B. tepikiense* is part of the *Gonyaulax–Spiniferites* clade. Work is in progress to try to reach a consensus on the nomenclature and taxonomy of the *Gonyaulax–Spiniferites* group, as well as the identity of the type species, *G. spinifera.*

Thirteen named species of *Spiniferites* have been more or less tentatively correlated with a motile stage in the *G. spinifera* group (Head 1996), but it is likely that many more species exist that have not yet been formally described. In the course of this study, we found many *Spiniferites* cysts that we were unable to identify, and some of these germinated to give unidentified motile cells (e.g. *Spiniferites* sp. from Japan, *Spiniferites* sp. from the Adriatic; our unpublished data).

In conclusion, it has been determined that separate cyst species germinate to produce separate and identifiable species of motile cells; this is confirmed by both morphological characters and LSU rDNA sequence. However, variation within species will make identification a challenge. At the generic level, doubts have now been raised about the validity of the genus *Bitectatodinium,* but further data are needed before a decision is reached on the systematics of this group.

REFERENCES

BOLCH C.J.S. 1997. The use of sodium polytungstate for the separation and concentration of living dinoflagellate cysts from marine sediments. *Phycologia* 36: 472–478.

DALE B. 1976. Cyst formation, sedimentation, and preservation: factors affecting dinoflagellate assemblages in Recent sediments from Trondheimsfjord, Norway. *Review of Palaeobotany and Palynology* 22: 39–60.

DALE B. 1978. Acritarchous cysts of *Peridinium faeroense* Paulsen: implications for dinoflagellate systematics. *Palynology* 2: 187–193.

DALE B. 1983. Dinoflagellate resting cysts: "benthic plankton." In: *Survival strategies of the algae* (Ed. by G.A. Fryxell), pp. 69–136. Cambridge University Press, Cambridge.

DALE B. 1996. Dinoflagellate cyst ecology – modeling and geological applications. In: *Palynology: principles and applications,* vol. 3 (Ed. by J. Jansonius & D.C. McGregor), pp. 1249–1275. American Association of Stratigraphic Palynologists, Houston, Texas.

DAUGBJERG N., MOESTRUP Ø. & ARCTANDER P. 1994. Phylogeny of the genus *Pyramimonas* (Prasinophyceae) inferred from the *rbc*L gene. *Journal of Phycology* 30: 991–999.

DAUGBJERG N., HANSEN G., LARSEN J. & MOESTRUP Ø. 2000. Phylogeny of some of the major genera of dinoflagellates based on ultrastructure and partial LSU rDNA sequence data, including the erection of three new genera of naked dinoflagellates. *Phycologia* 39: 302–317.

DOYLE J.J. & DOYLE J.L. 1987. A rapid DNA isolation procedure for small quantities of fresh leaf tissue. *Phytochemical Bulletin* 19: 11–15.

ELLEGAARD M., LEWIS J. & HARDING I. 2002. *Gonyaulax baltica* sp. nov. (Dinophyceae) – cyst–theca relationship, life cycle and environmentally induced morphological variations in the cyst of a new species from The Baltic. *Journal of Phycology* 38: 775–789.

FAURÉ-FREMIET E. 1908. Étude descriptive des Péridiens et des infusoires ciliés du plankton de la Baie de la Hougue. *Annales des Sciences Naturelles Zoologie* 9(7): 209–243.

FELSENSTEIN J. 1985. Confidence limits on phylogenies: an approach using the bootstrap. *Evolution* 39: 783–791.

FENSOME R.A., TAYLOR F.J.R., NORRIS G., SARJEANT W.A.S., WHARTON D.I. & WILLIAMS G.L. 1993. A classification of living and fossil dinoflagellates. *Micropaleontology,* Special Publication 7: 1–351.

FRITZ L. & TREIMER R.E. 1985. A rapid simple technique utilizing Calcofluor White MR2 for the visualization of dinoflagellate thecal plates. *Journal of Phycology* 21: 662–664.

GREUTER W., McNEILL J., BARRIE F.R., BURDET H.M., DEMOULIN V., FILGUEIRAS T.S., NICOLSON D.H., SILVA P.C., SKOG J.E., TREHANE P., TURLAND N.J. & HAWKSWORTH D.L. 2000. *International Code of Botanical Nomenclature (Saint Louis Code).* Koeltz Scientific Books, Königstein, Germany. 474 pp.

GUILLARD R.R.L. 1973. Methods for microflagellates and nanoplankton. In: *Handbook of phycological methods, culture methods and growth measurements* (Ed. by J.R. Stein), pp. 69–85. Cambridge University Press, Cambridge.

HALLETT R. 1999. *Consequences of environmental change on the growth and morphology of* Lingulodinium polyedrum *(Dinophyceae) in culture.* PhD thesis. University of Westminster, London. 145 pp.

HANSEN G. 1993. Dimorphic individuals of *Dinophysis acuta* and *D. norvegica* (Dinophyceae) from Danish waters. *Phycologia* 32: 73–75.

HANSEN G., DAUGBJERG N. & HENRIKSEN P. 2000. Comparative study of *Gymnodinium mikimotoi* and *Gymnodinium aureolum,* comb. nov. (= *Gyrodinium aureolum*) based on morphology, pigment composition, and molecular data. *Journal of Phycology* 36: 394–410.

HARLAND R. 1982a. Recent dinoflagellate cyst assemblages from the southern Barents Sea. *Palynology* 6: 9–18.

HARLAND R. 1982b. A review of Recent and Quaternary organic-walled dinoflagellate cysts of the genus *Protoperidinium. Palaeontology* 25: 369–397.

HARLAND R. 1983. Distribution maps of Recent dinoflagellate cysts in bottom sediments from the North Atlantic Ocean and adjacent seas. *Palaeontology* 26: 321–387.

HARLAND R. & DOWNIE C. 1969. The dinoflagellates of the interglacial deposits at Kirmington, Lincolnshire. *Proceedings of the Yorkshire Geological Society* 37: 231–237.

HARLAND R. & SHARP J. 1986. Elongate *Spiniferites* cysts from North Atlantic bottom sediments. *Palynology* 10: 25–34.

HARLAND R., REID P.C., DOBELL P. & NORRIS G. 1980. Recent and sub-Recent dinoflagellate cysts from the Beaufort Sea, Canadian Arctic. *Grana* 19: 211–225.

HEAD M.J. 1996. Modern dinoflagellate cysts and their biological affinities. In: *Palynology: principles and applications,* vol. 3 (Ed. by J. Jansonius & D.C. McGregor), pp. 1197–1248. American Association of Stratigraphic Palynologists Foundation, Houston, Texas.

KOFOID C.A. 1911. Dinoflagellata of the San Diego region, IV. The genus *Gonyaulax,* with notes on its skeletal morphology and a discussion of its generic and specific characters. *University of California Publications in Zoology* 8: 187–286.

LENAERS G., MAROTEAUX L., MICHOT B. & HERZOG M. 1989. Dinoflagellates in evolution. A molecular phylogenetic analysis of large subunit ribosomal RNA. *Journal of Molecular Evolution* 29: 40–51.

LEWIS J. 1991. Cyst–theca relationships in *Scrippsiella* (Dinophyceae) and related orthoperidinioid genera. *Botanica Marina* 34: 91–106.

LEWIS J., ROCHON A. & HARDING I. 1999. Preliminary observations of cyst–theca relationships in *Spiniferites ramosus* and *Spiniferites membranaceus* (Dinophyceae). *Grana* 38: 113–124.

LEWIS J., ROCHON A., ELLEGAARD M., MUDIE P. & HARDING I. 2001. The cyst–theca relationship of *Bitectatodinium tepikiense* (Dinophyceae). *European Journal of Phycology* 36: 137–146.

MATSUOKA K. 1987. Organic-walled dinoflagellate cysts from surface sediments of Akkeshi Bay and Lake Saroma, North Japan. *Bulletin of the Faculty of Liberal Arts, Nagasaki University, Natural Science* 28: 35–123.

MATSUOKA K. 1992. Species diversity of modern dinoflagellate cysts in surface sediments around the Japanese Islands. In: *Neogene and Quaternary dinoflagellate cysts and acritarchs* (Ed. by M.J. Head & J.H. Wrenn), pp. 33–53. American Association of Stratigraphic Palynologists Foundation, Dallas, Texas.

NEHRING S. 1997. Dinoflagellate resting cysts from Recent German coastal sediments. *Botanica Marina* 40: 307–324.

REID P.C. 1974. Gonyaulacacean dinoflagellate cysts from the British Isles. *Nova Hedwigia* 25: 579–637.

ROCHON A., DE VERNAL A., TURON J.-L., MATTHIESSEN J. & HEAD M.J. 1999. *Distribution of Recent dinoflagellate cysts in surface sediments from the North Atlantic Ocean and adjacent seas in relation to sea-surface parameters.* Contribution Series Number 35. American Association of Stratigraphic Palynologists Foundation, Dallas. 152 pp.

ROSSIGNOL M. 1964. Hystrichosphères du quaternaire en Méditerranée orientale, dans les sédiments pléistocènes et les boues marines actuelles. *Revue de Micropaléontologie* 7: 83–99.

SCHOLIN C.A., HERZOG M., SOGIN M. & ANDERSON D.M. 1994. Identification of group- and stain-specific markers for globally distributed *Alexandrium* (Dinophyceae). II. Sequence analysis of a fragment of the LSU rRNA gene. *Journal of Phycology* 30: 999–1011.

SCHOLIN C.A., HALLEGRAEFF G.M. & ANDERSON D.M. 1995. Molecular evolution of the *Alexandrium tamarense* 'species complex' (Dinophyceae): dispersal in the North American and west Pacific regions. *Phycologia* 43: 472–485.

SWOFFORD D.L. 1998. *PAUP* – phylogenetic analysis using parsimony (*and other methods), version 4.* Sinauer Associates, Sunderland, Massachusetts.

WALL D. & DALE B. 1968. Modern dinoflagellate cysts and evolution of the Peridiniales. *Micropaleontology* 14: 265–304.

WALL D., DALE B., LOHMANN G.P. & SMITH W.K. 1977. The environmental and climatic distribution of dinoflagellate cysts in modern marine sediments from regions in the North and South Atlantic Oceans and adjacent seas. *Marine Micropaleontology* 2: 121–200.

WILLIAMS G.L., LENTIN J.K. & FENSOME R.A. 1998. *The Lentin and Williams index of fossil dinoflagellates 1998 edition.* Contribution Series Number 34. American Association of Stratigraphic Palynologists, Dallas. 817 pp.

WILLIAMS G.L., FENSOME R.A., MILLER M.A. & SARJEANT W.A.S. 2000. *A glossary of the terminology applied to dinoflagellates, acritarchs and prasinophytes, with emphasis on fossils,* ed. 3. Contribution Series Number 37, American Association of Stratigraphic Palynologists, Dallas. 370 pp.

WUYTS J., DE RIJK P., VAN DE PEER Y., WINKELMANS T. & DE WACHTER R. 2001. The European large subunit ribosomal RNA database. *Nucleic Acids Research* 29: 175–177.